

6-1-1997

## Degenerate Layer at GaN/Sapphire Interface: Influence on Hall-Effect Measurements

David C. Look

Wright State University - Main Campus, david.look@wright.edu

Richard J. Molnar

Follow this and additional works at: <https://corescholar.libraries.wright.edu/physics>



Part of the [Physics Commons](#)

---

### Repository Citation

Look, D. C., & Molnar, R. J. (1997). Degenerate Layer at GaN/Sapphire Interface: Influence on Hall-Effect Measurements. *Applied Physics Letters*, 70 (25), 3377-3379.  
<https://corescholar.libraries.wright.edu/physics/57>

This Article is brought to you for free and open access by the Physics at CORE Scholar. It has been accepted for inclusion in Physics Faculty Publications by an authorized administrator of CORE Scholar. For more information, please contact [library-corescholar@wright.edu](mailto:library-corescholar@wright.edu).

# Degenerate layer at GaN/sapphire interface: Influence on Hall-effect measurements

D. C. Look

University Research Center, Wright State University Dayton, Ohio 45435

R. J. Molnar

Lincoln Laboratory, Massachusetts Institute of Technology, Lexington, Massachusetts 02173

(Received 13 March 1997; accepted for publication 16 April 1997)

Temperature-dependent Hall-effect measurements in hydride vapor phase epitaxial GaN grown on sapphire can be well fitted over the temperature range 10–400 K by assuming a thin, degenerate  $n$ -type region at the GaN/sapphire interface. This degenerate interfacial region dominates the electrical properties below 30 K, but also significantly affects those properties even at 400 K, and can cause a second, deeper donor to falsely appear in the analysis. However, by using a two-layer Hall model, the bulk mobility and carrier concentration can be accurately ascertained. © 1997 American Institute of Physics. [S0003-6951(97)00125-3]

Progress in GaN materials<sup>1</sup> and device development<sup>2</sup> has accelerated in the past few years following the demonstration of high-conductivity,  $p$ -type epitaxial layers.<sup>3</sup> Blue light-emitting diodes are already a commercial product,<sup>4</sup> and blue laser diodes,<sup>5</sup> uv detectors,<sup>6</sup> and high-power, high-temperature field-effect transistors<sup>7</sup> have been demonstrated and are improving rapidly. Most of the GaN (also InGaN and AlGaIn) material used so far for device development consists of epitaxial growth on sapphire, and the epitaxial techniques include metalorganic chemical vapor deposition (MOCVD), molecular beam epitaxy (MBE) and hydride vapor phase epitaxy (HVPE). Because of the large lattice mismatch (14%) between GaN and sapphire, a thin, highly dislocated region is generated at the layer/substrate interface to relieve the strain, and the structural properties of this interface region have been studied in great detail. However, little is known about the electrical and optical properties of the interface. Recently, Götz *et al.*<sup>8</sup> have progressively thinned a 13- $\mu\text{m}$ -thick HVPE layer down to 1.2  $\mu\text{m}$ , and shown that the conductance does not scale down linearly, but that a significant component must exist at or near the interface. In the present work, we show by temperature-dependent Hall-effect measurements and theory that this interface conductance can be quantified, nondestructively, and that it significantly affects the usual fits of carrier concentration versus temperature. That is, without correction, the fitted shallow donor concentration is too large and its energy is too low; furthermore, a second, deeper donor often falsely appears. The mobility versus temperature curve is also affected in that the whole curve is shifted downward from the true, bulk curve. Fortunately, both carrier concentration and mobility data can be corrected by a two-layer Hall analysis.<sup>9</sup>

The GaN sample, 289B, was grown by hydride vapor phase epitaxy on sapphire to a thickness of 20  $\mu\text{m}$ . Sputtered ZnO was used as a buffer layer between the sapphire and GaN, but the ZnO was no longer present after completion of the growth.<sup>10</sup> In the study described in Ref. 8, GaCl was used instead of ZnO in the pretreatment process; however, our results described below are nearly identical for the two types of pretreatments. It is known that the GaCl-pretreated interface contains a thin (2000–3000 Å), high-density region of

stacking faults; the same may also be true for the ZnO-pretreated interface.

By performing Hall measurements as the layer thickness in their sample was reduced from 13 to 1.2  $\mu\text{m}$ , Götz *et al.*<sup>8</sup> estimated that the sheet concentration of donors in the interfacial region exceeded  $10^{15} \text{ cm}^{-2}$ . Capacitance-voltage measurements, on the other hand, showed that  $N_D - N_A$  was relatively constant at about  $5 \times 10^{16} \text{ cm}^{-3}$ , which would give a sheet concentration of only about  $7 \times 10^{13} \text{ cm}^{-2}$  for the whole, 13  $\mu\text{m}$  layer. Thus, Götz *et al.* concluded that the Hall measurements were strongly affected by the interfacial region, but they did not determine how to obtain the correct bulk electrical data in the presence of this effect. Here we quantitatively elucidate both the bulk and interfacial electrical properties by applying a two-layer Hall-effect model to the temperature-dependent conductivity ( $\sigma$ ) and Hall-coefficient ( $R$ ) data. It is critical in this analysis to get experimental data below 30 K, because the interfacial layer begins to dominate at this temperature.

The relevant relationships for a multiband (or multilayer) analysis are<sup>9</sup>

$$\sigma_{\square} = \sum_i \sigma_{\square i} = \sum_i e \mu_i n_{\square i} = \sum_i e \mu_{Hi} n_{H\square i}, \quad (1)$$

$$R_{\square} \sigma_{\square}^2 = \sum_i R_{\square i} \sigma_{\square i}^2 = \sum_i e \mu_{Hi}^2 n_{H\square i}, \quad (2)$$

where  $\mu_i$  is the conductivity mobility of layer  $i$ ,  $\mu_{Hi}$  ( $= R_{\square i} \sigma_{\square i}$ ) is the Hall mobility,  $n_{\square i}$  is the true sheet carrier concentration, and  $n_{H\square i}$  ( $= n_{\square i} / r_i$ ) is the sheet Hall concentration, where  $r_i$  is the Hall factor. Note that the symbol “ $\square$ ” denotes a sheet concentration ( $\text{cm}^{-2}$ ), rather than a volume concentration ( $\text{cm}^{-3}$ ). (It should be remembered that a simple Hall measurement gives no thickness information, and thus can determine only sheet concentration.) Our case is a two-layer problem, with  $i=1$  representing the bulk layer, and  $i=2$ , the interfacial layer. For plotting purposes, we normalize both layers to the bulk thickness,  $d=20 \mu\text{m}$ ; i.e., we divide Eqs. (1) and (2) by  $d$ . Then, in terms of the normally measured quantities,  $\mu_H$  and  $n_H$ , we get

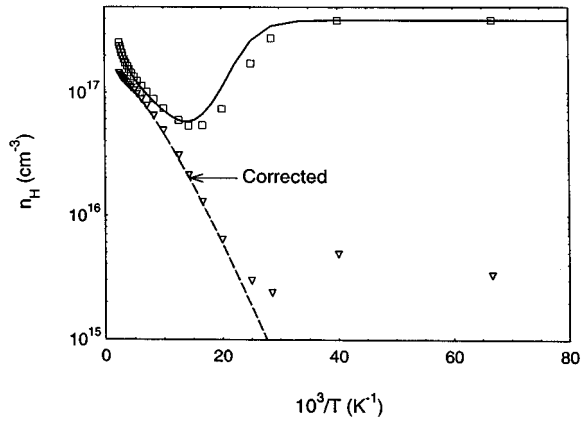


FIG. 1. Uncorrected Hall concentration data (squares) and fit (solid line), and corrected data (triangles) and fit (dashed line) vs inverse temperature.

$$\mu_H = R_{\square} \sigma_{\square} = \frac{R_{\square} \sigma_{\square}^2 / d}{\sigma_{\square} / d} = \frac{\mu_{H1}^2 n_{H1} + \mu_{H2}^2 n_{H_{\square 2}} / d}{\mu_{H1} n_{H1} + \mu_{H2} n_{H_{\square 2}} / d}, \quad (3)$$

$$\begin{aligned} n_H &= \frac{n_{H_{\square}}}{d} = \frac{1}{e R_{\square} d} \\ &= \frac{\sigma_{\square}^2 / d^2}{e R_{\square} \sigma_{\square}^2 / d} \\ &= \frac{(\mu_{H1} n_{H1} + \mu_{H2} n_{H_{\square 2}} / d)^2}{\mu_{H1}^2 n_{H1} + \mu_{H2}^2 n_{H_{\square 2}} / d}. \quad (4) \end{aligned}$$

The Hall concentration and Hall mobility data are presented in Figs. 1 and 2, respectively. Beginning at high  $T$  (low  $1/T$ ) and proceeding toward low  $T$ , we see a classic donor freeze out in Fig. 1, which suggests that the bulk concentration,  $n_{H1}$ , is negligible at the lowest values of  $T$ . Thus, at very low  $T$ , the interfacial layer must be dominant so that  $\mu_H = \mu_{H2}$  and  $n_H = n_{H_{\square 2}} / d$ . Both the mobility and carrier concentration data are flat below 30 K, denoting a degenerate layer. From Fig. 2,  $\mu_{H2} = 55 \text{ cm}^2/\text{V s}$ , and from Fig. 1,  $n_{H_{\square 2}} / d = 3.9 \times 10^{17} \text{ cm}^{-3}$ , or  $n_{H_{\square 2}} \approx 8 \times 10^{14} \text{ cm}^{-2}$ . Note that this value is quite comparable to the estimate of Gotz *et al.*,<sup>8</sup> mentioned earlier, even though their GaN layer was grown with a different (GaCl) pretreatment. To further validate that  $n_{H_{\square 2}}$  represents the interfacial layer, we took data

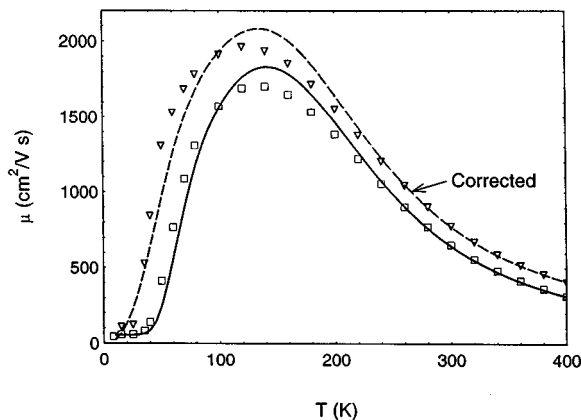


FIG. 2. Uncorrected Hall mobility data (squares) and fit (solid line), and corrected data (triangles) and fit (dashed line) vs temperature.

on a different sample, 262D, which was  $60 \mu\text{m}$  thick but also grown on sapphire with a ZnO pretreatment. For this latter layer,  $n_{H_{\square 2}} = 7 \times 10^{14} \text{ cm}^{-2}$ , which is in excellent agreement. Thus, low- $T$  Hall measurements provide a useful way to characterize the GaN/sapphire interface. If the source of interfacial electrons is the  $2000 \text{ \AA}$  highly defected region, then the volume density of electrons in this region is  $n_{H2} = n_{H_{\square 2}} / 2000 \text{ \AA} \approx 4 \times 10^{19} \text{ cm}^{-3}$ . Clearly, this electron concentration would be expected to be degenerate and temperature-independent (as observed), since the Mott concentration<sup>11</sup> in GaN is about  $1 \times 10^{18} \text{ cm}^{-3}$ , and the concentration at which the Fermi level enters the conduction band,<sup>12</sup> about  $6 \times 10^{18} \text{ cm}^{-3}$ . Thus, our model is self-consistent. Note that because the layer is degenerate,  $n_2 = n_{H2}$ ; i.e.,  $r_2$ , the Hall  $r$  factor will be close to unity.

The temperature independence of  $\mu_2$  and  $n_2$  allows an easy separation of the bulk properties,  $n_{H1}$  and  $\mu_{H1}$ , from the two-layer properties,  $n_H$  and  $\mu_H$ :

$$\mu_{H1} = \frac{\mu_H^2 n_H - \mu_2^2 n_{\square 2} / d}{\mu_H n_H - \mu_2 n_{\square 2} / d}, \quad (5)$$

$$n_{H1} = \frac{(\mu_H n_H - \mu_2 n_{\square 2} / d)^2}{\mu_H^2 n_H - \mu_2^2 n_{\square 2} / d}. \quad (6)$$

We plot the extracted  $n_{H1}$  and  $\mu_{H1}$  in Figs. 1 and 2, respectively. Several interesting features are immediately noticed: (1) the carrier concentration and mobility data are affected over the full temperature range, not just at low temperature; (2) the  $n_{H1}$  vs  $T$  data look like they represent a standard, single-donor case, whereas if we had considered the uncorrected ( $n_H$ ) data only, in the usual temperature range  $T = 80\text{--}400 \text{ K}$  (or  $10^3/T = 12.5\text{--}2.5$ ), we would have had to use a two-donor model to fit the data; and (3) the true 300 K Hall mobility ( $\mu_{H1}$ ), which is often used as a figure of merit, is significantly higher ( $784$  vs  $633 \text{ cm}^2/\text{V s}$ ) than that given by the uncorrected data ( $\mu_H$ ).

To fit the carrier-concentration data, we use a single-donor model<sup>13</sup>

$$n + N_A = \frac{N_D}{1 + n/\phi}, \quad (7)$$

where  $\phi = g_0 / g_1 N'_C T^{3/2} \exp(-E_D/kT)$ . Here  $N_D$  is the donor concentration,  $N_A$  the acceptor concentration,  $g_0$  the degeneracy of the unoccupied donor state (assume  $g_0 = 1$ ),  $g_1$  the degeneracy of the occupied state (assume  $g_1 = 2$ ),  $N'_C$ , the effective density of states at  $T = 1 \text{ K}$  ( $N'_C \approx 4.98 \times 10^{14} \text{ cm}^{-3}$  for  $m^* = 0.22m_0$ ), and  $E_D$  the donor activation energy. The parameters fitted from Eq. (7) include only  $N_D$  and  $E_D$ , since  $N_A$  is determined from the mobility fit.

The mobility is fitted by solving the Boltzmann equation in the relaxation-time approximation.<sup>14</sup> That is,  $\mu_H = e \langle \tau^2 \rangle / m^* \langle \tau \rangle$ , where the brackets denote an average over electron energy  $E$ , and

$$\frac{1}{\tau(E)} = \frac{1}{\tau_{ac}(E)} + \frac{1}{\tau_{po}(E)} + \frac{1}{\tau_{pe}(E)} + \frac{1}{\tau_{ii}(E)}. \quad (8)$$

The terms in Eq. (8) represent the usual acoustic mode, polar-optical mode, piezoelectric, and ionized-impurity (or defect) scattering, respectively. In actuality, an analytical

form for  $\tau_{po}(E)$  cannot be written, because the scattering is inelastic; however, following a treatment similar to that discussed in Ref. 14, we can write an analytical expression for  $\tau_{po}(E)$  that approximately reproduces the polar-optical mobility found by an iterative solution of the Boltzmann equation. We have shown that the fitted  $N_A$  varies little by invoking the relaxation-time approximation, but that the computational time is much less. The rest of the scattering constants are taken from the literature:<sup>15</sup> acoustic-deformation potential,  $E_1=9.2$  eV; piezoelectric constant,  $\epsilon_{14}=0.5$  C/m<sup>2</sup>; low-frequency dielectric constant,  $\epsilon_{lf}=10.4\epsilon_0$ ; high-frequency dielectric constant,  $\epsilon_{hf}=5.47\epsilon_0$ ; Debye temperature,  $T_D=1044$  K; and effective mass,  $m^*=0.22m_0$ . Also, the polar-optical scattering was increased by a factor of 1.8 in order to fit the high-temperature part of the mobility curve. However, this factor has little effect on the low-temperature region, where ionized-impurity scattering dominates, so that a reliable value of  $N_A$  can still be calculated.

The fits are shown as solid lines (for  $n_H$  and  $\mu_H$ ) and dashed lines (for  $n_{H1}$  and  $\mu_{H1}$ ) in Figs. 1 and 2. Clearly, the fits are satisfactory and verify the model. The fitting parameters are:  $N_D=2.1\times 10^{17}$  cm<sup>-3</sup>,  $N_A=5\times 10^{16}$  cm<sup>-3</sup>, and  $E_D=16$  meV. If the donor is Si, which presumably has a donor energy of  $E_{D0}=29$  meV,<sup>16</sup> at  $N_D=0$ , then we would expect  $E_D=E_{D0}-\alpha N_D^{1/3}=16.5$  meV, since  $\alpha$  (the screening factor) has been given as  $2.1\times 10^{-5}$  meV cm.<sup>17</sup> Although our fitted  $E_D$  is in excellent agreement, it should not be taken as a verification of  $E_{D0}$  or  $\alpha$ ; much more work on many other samples will be necessary to establish these two parameters accurately. In fact, a value of  $E_{D0}=35$  meV for residual donors (perhaps Si) has also been suggested.<sup>17</sup>

A final confirmation of our analysis comes from 300 K capacitance-voltage measurements, which give a concentration of  $1.2\times 10^{17}$  cm<sup>-3</sup> in the near-surface (0.1–0.3  $\mu$ m) region. This value is close to the corrected Hall concentration of  $1.3\times 10^{17}$  cm<sup>-3</sup>, but far from the uncorrected concentration of  $1.9\times 10^{17}$  cm<sup>-3</sup>.

In summary, we have shown that HVPE GaN layers grown directly on sapphire contain a thin, highly degenerate  $n$ -type region which is close to the GaN/sapphire interface and is likely associated with a 2000 Å region of high-density stacking faults, reported earlier. For the present sample,  $n\approx 8\times 10^{14}$  cm<sup>-2</sup> and  $\mu\approx 55$  cm<sup>2</sup>/V s in this region. This degenerate layer significantly affects the mobility and carrier

concentration data, even at high temperatures. However, a simple two-layer Hall-effect model fits both the mobility and carrier-concentration data very well, and allows the bulk electrical parameters to be extracted. In particular, the true 300 K mobility, often used as a figure of merit, is significantly higher than that given by the uncorrected data.

The authors would like to thank T. A. Cooper for Hall-effect measurements, Z-Q. Fang for capacitance-voltage measurements, G. D. Via for metallization, D. C. Reynolds, J. R. Sizelove, R. L. Jones, C. E. Stutz, C. W. Litton, H. Morkoç for helpful discussions, and R. Heil for manuscript preparation. The work of DCL was performed at the Avionics Directorate of Wright Laboratory, Wright-Patterson Air Force Base, under Contract No. F33615-95-C-1619. The work of RJM was supported by DARPA and the Department of the Air Force. Opinions, interpretations, conclusions, and recommendations are those of the authors, and are not necessarily endorsed by the U.S. Air Force.

<sup>1</sup>For a materials review, see S. Strite and H. Morkoç, *J. Vac. Sci. Technol. B* **10**, 1237 (1992).

<sup>2</sup>For a device review, see S. N. Mohammad, A. A. Salvador, and H. Morkoç, *Proc. IEEE* **83**, 1306 (1995).

<sup>3</sup>H. Amano, M. Kito, K. Hiamatsu, and I. Akasaki, *Jpn. J. Appl. Phys.* **28**, L2112 (1989).

<sup>4</sup>S. Nakamura, M. Senoh, N. Iwasa, and S. Nagahama, *Appl. Phys. Lett.* **67**, 1869 (1995).

<sup>5</sup>S. Nakamura, M. Senoh, S. Nagahama, N. Iwasa, T. Yamada, T. Matsushita, H. Kiyoka, and Y. Sugimoto, *Jpn. J. Appl. Phys.* **35**, L74 (1996).

<sup>6</sup>M. Razeghi and A. Rogalski, *J. Appl. Phys.* **79**, 7433 (1996).

<sup>7</sup>M. A. Khan, Q. Chen, M. S. Shur, B. T. Dermott, J. A. Higgins, J. Burm, W. J. Schaff, and L. F. Eastman, *IEEE Electron Device Lett.* **17**, 584 (1996).

<sup>8</sup>W. Götz, J. Walker, L. T. Romano, N. M. Johnson, and R. J. Molnar, *Mater. Res. Soc. Symp. Proc.* **449**, 525 (1997).

<sup>9</sup>D. C. Look, *Electrical Characterization of GaAs Materials and Devices* (Wiley, New York, 1989), App. B.

<sup>10</sup>R. J. Molnar, K. B. Nichols, P. Makai, E. R. Brown, and I. Melngailis, *Mater. Res. Soc. Symp. Proc.* **378**, 479 (1995).

<sup>11</sup>N. F. Mott and W. D. Twose, *Adv. Phys.* **10**, 107 (1961).

<sup>12</sup>T. Matsubara and Y. Toyozawa, *Prog. Theor. Phys.* **26**, 739 (1961).

<sup>13</sup>D. C. Look, *Electrical Characterization of GaAs Materials and Devices* (Wiley, New York, 1989), p. 116.

<sup>14</sup>D. C. Look, *Electrical Characterization of GaAs Materials and Devices* (Wiley, New York, 1989), p. 93.

<sup>15</sup>The various references are summarized in D. C. Look, J. R. Sizelove, S. Keller, Y. F. Wu, U. K. Mishra, and S. P. DenBaars, *Solid State Commun.* **102**, 297 (1997).

<sup>16</sup>Y. J. Wang, R. Kaplan, H. K. Ng, K. Doverspike, D. K. Gaskill, T. Ikeda, H. Amano, and I. Akasaki, *J. Appl. Phys.* **79**, 8007 (1996).

<sup>17</sup>B. K. Meyer, D. Volm, A. Graber, H. C. Alt, T. Detchprohm, A. Amano, and I. Akasaki, *Solid State Commun.* **95**, 597 (1995).